Sampling Conditions for Clipping-free Voronoi Meshing by the VoroCrust Algorithm

Scott Mitchell[1], Ahmed Abdelkader[2], Ahmad Rushdi[3], Mohamed Ebeida[1], Ahmed Mahmoud[3], John Owens[3] and Chandrajit Bajaj[4]

[1]Sandia National Laboratories

[2]University of Maryland, College Park

[3]University of California, Davis

[4]University of Texas, Austin

Introduction

Voronoi Meshing

Given a bounded open set $\mathcal{O}$ in Euclidean space, decompose its interior into Voronoi cells of bounded aspect-ratio. The cells should naturally *conform* to the bounding surface $\mathcal{M} = \partial\mathcal{O}$.

Introduction

Voronoi Meshing

Given a bounded open set $\mathcal{O}$ in Euclidean space, decompose its interior into Voronoi cells of bounded aspect-ratio. The cells should naturally *conform* to the bounding surface $\mathcal{M} = \partial\mathcal{O}$.

- To the best of our knowledge, this stands as an open problem for non-convex domains.

Introduction

Voronoi Meshing

Given a bounded open set $\mathcal{O}$ in Euclidean space, decompose its interior into Voronoi cells of bounded aspect-ratio. The cells should naturally *conform* to the bounding surface $\mathcal{M} = \partial\mathcal{O}$.

- To the best of our knowledge, this stands as an open problem for non-convex domains.
- This is in contrast with tetrahedral meshing, which is well-established.

Introduction

Voronoi Meshing

Given a bounded open set $\mathcal{O}$ in Euclidean space, decompose its interior into Voronoi cells of bounded aspect-ratio. The cells should naturally *conform* to the bounding surface $\mathcal{M} = \partial\mathcal{O}$.

- To the best of our knowledge, this stands as an open problem for non-convex domains.
- This is in contrast with tetrahedral meshing, which is well-established.
- The VoroCrust project developed the first solution to this problem.

Introduction

Voronoi Meshing

Given a bounded open set $\mathcal{O}$ in Euclidean space, decompose its interior into Voronoi cells of bounded aspect-ratio. The cells should naturally *conform* to the bounding surface $\mathcal{M} = \partial\mathcal{O}$.

- To the best of our knowledge, this stands as an open problem for non-convex domains.
- This is in contrast with tetrahedral meshing, which is well-established.
- The VoroCrust project developed the first solution to this problem.
- In this talk, we focus on the subproblem of surface reconstruction, assuming a set of sample points from $\mathcal{M}$ is given as input.

Problem Definition and State-of-the-art

Surface Reconstruction for Voronoi Meshing

Given a set of sample points from a closed 2-manifold $\mathcal{M}$ in Euclidean space, decompose its interior into Voronoi cells of bounded aspect-ratio. The cells should naturally *conform* to a surface mesh approximating $\mathcal{M}$.

Problem Definition and State-of-the-art

Surface Reconstruction for Voronoi Meshing

Given a set of sample points from a closed 2-manifold $\mathcal{M}$ in Euclidean space, decompose its interior into Voronoi cells of bounded aspect-ratio. The cells should naturally *conform* to a surface mesh approximating $\mathcal{M}$.

- Typically, cells near the boundary are *clipped*, introducing defects.

Problem Definition and State-of-the-art

Surface Reconstruction for Voronoi Meshing

Given a set of sample points from a closed 2-manifold $\mathcal{M}$ in Euclidean space, decompose its interior into Voronoi cells of bounded aspect-ratio. The cells should naturally *conform* to a surface mesh approximating $\mathcal{M}$.

- Typically, cells near the boundary are *clipped*, introducing defects.
- Power crust [Amenta et al.] produces such a decomposition. However,

Problem Definition and State-of-the-art

Surface Reconstruction for Voronoi Meshing

Given a set of sample points from a closed 2-manifold $\mathcal{M}$ in Euclidean space, decompose its interior into Voronoi cells of bounded aspect-ratio. The cells should naturally *conform* to a surface mesh approximating $\mathcal{M}$.

- Typically, cells near the boundary are *clipped*, introducing defects.
- Power crust [Amenta et al.] produces such a decomposition. However,
    - Generators (poles) are restricted to lie near the medial axis of $\mathcal{M}$.

Problem Definition and State-of-the-art

Surface Reconstruction for Voronoi Meshing

Given a set of sample points from a closed 2-manifold $\mathcal{M}$ in Euclidean space, decompose its interior into Voronoi cells of bounded aspect-ratio. The cells should naturally *conform* to a surface mesh approximating $\mathcal{M}$.

- Typically, cells near the boundary are *clipped*, introducing defects.
- Power crust [Amenta et al.] produces such a decomposition. However,
  - Generators (poles) are restricted to lie near the medial axis of $\mathcal{M}$.
  - Instead of the Voronoi diagram, it is based on the power diagram.

Problem Definition and State-of-the-art

Surface Reconstruction for Voronoi Meshing

Given a set of sample points from a closed 2-manifold $\mathcal{M}$ in Euclidean space, decompose its interior into Voronoi cells of bounded aspect-ratio. The cells should naturally *conform* to a surface mesh approximating $\mathcal{M}$.

- Typically, cells near the boundary are *clipped*, introducing defects.
- Power crust [Amenta et al.] produces such a decomposition. However,
  - Generators (poles) are restricted to lie near the medial axis of $\mathcal{M}$.
  - Instead of the Voronoi diagram, it is based on the power diagram.
  - Nonetheless, rich theory with strong approximation guarantees.

VoroCrust Intuition - A 2D Example

(1) Weighted samples (balls)

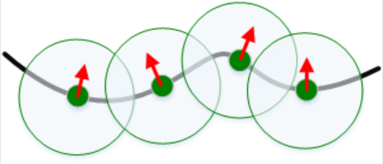

VoroCrust Intuition - A 2D Example

(1) Weighted samples (balls)

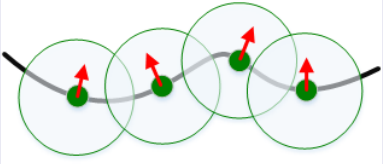

(2) Collect intersection points

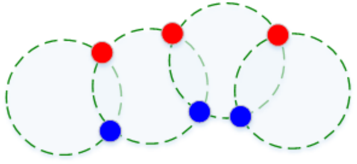

VoroCrust Intuition - A 2D Example

(1) Weighted samples (balls)

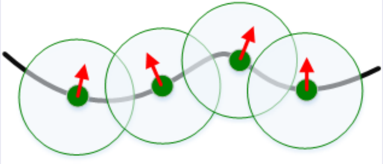

(2) Collect intersection points

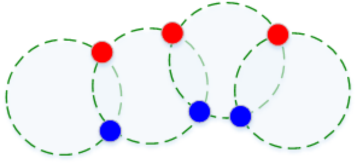

(3) Compute Voronoi diagram

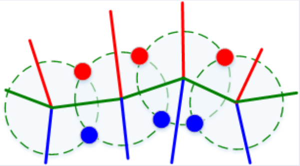

VoroCrust Intuition - A 2D Example

(1) Weighted samples (balls)

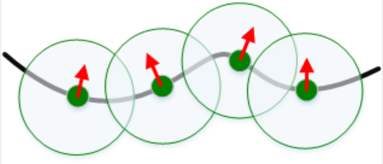

(2) Collect intersection points

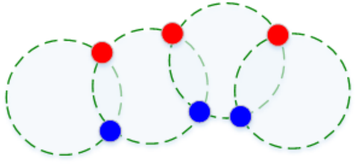

(3) Compute Voronoi diagram

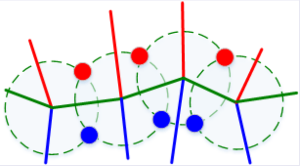

(4) Keep the separating facets

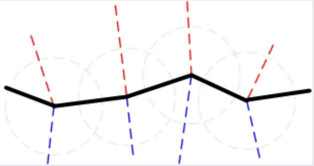

The Union of Balls and Its Dual Shape [Edelsbrunner]

Power distance and cell

For a ball b centered at c with radius r, $\pi(b, x) = \|cx\|^2 - r^2$.
$V_b = \{x \in \mathbb{R}^d \mid \pi(b, x) \leq \pi(b', x) \, \forall b' \in B\}$.

The Union of Balls and Its Dual Shape [Edelsbrunner]

Power distance and cell

For a ball b centered at c with radius r, $\pi(b, x) = \|cx\|^2 - r^2$.
$V_b = \{x \in \mathbb{R}^d \mid \pi(b, x) \leq \pi(b', x)\ \forall b' \in B\}$.

Weighted α-complex and α-shape

Define $\mathcal{K} = Nerve(\{V_b \cap b \mid b \in B\})$ and $\mathcal{S}$ as the underlying space $|\mathcal{K}|$.

The Union of Balls and Its Dual Shape [Edelsbrunner]

Power distance and cell

For a ball b centered at c with radius r, $\pi(b, x) = \|cx\|^2 - r^2$.
$V_b = \{x \in \mathbb{R}^d \mid \pi(b, x) \leq \pi(b', x)\ \forall b' \in B\}$.

Weighted α-complex and α-shape

Define $\mathcal{K} = Nerve(\{V_b \cap b \mid b \in B\})$ and $\mathcal{S}$ as the underlying space $|\mathcal{K}|$.

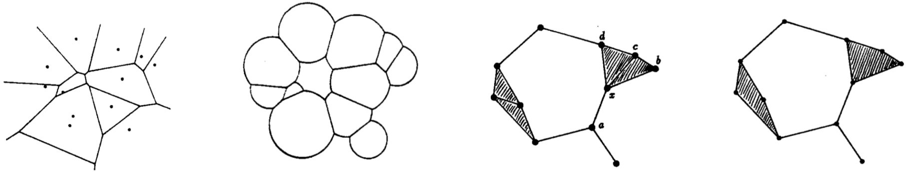

Figures from [Edelsbrunner]

The Union of Balls and Its Dual Shape [Edelsbrunner]

Power distance and cell

For a ball b centered at c with radius r, $\pi(b, x) = \|cx\|^2 - r^2$.
$V_b = \{x \in \mathbb{R}^d \mid \pi(b, x) \leq \pi(b', x)\ \forall b' \in B\}$.

Weighted α-complex and α-shape

Define $\mathcal{K} = Nerve(\{V_b \cap b \mid b \in B\})$ and $\mathcal{S}$ as the underlying space $|\mathcal{K}|$.

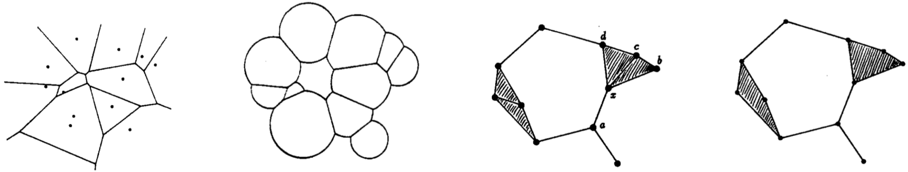

Figures from [Edelsbrunner]

Homotopy-equivalence

The nerve theorem implies $\mathcal{S} = |\mathcal{K}|$ has the same homotopy-type as $\cup B$.

ϵ-Sampling and Topological Thickening

Local features size (lfs)

The local feature size at a point $x \in \mathcal{M}$ is its distance to the medial axis of $\mathcal{M}$.

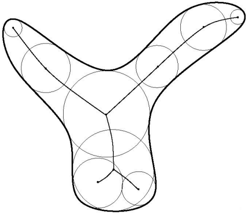

Medial Axis
Figure from [Wolter]

ϵ-Sampling and Topological Thickening

Local features size (lfs)

The local feature size at a point $x \in \mathcal{M}$ is its distance to the medial axis of $\mathcal{M}$.

ϵ-sample

A set of points P on $\mathcal{M}$ such that $\forall x \in \mathcal{M}\ \exists p \in P$ s.t. $||px|| \leq \epsilon \cdot lfs(x)$.

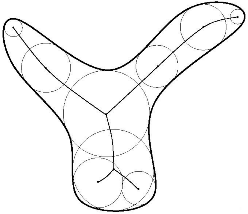

Medial Axis
Figure from [Wolter]

ϵ-Sampling and Topological Thickening

Local features size (lfs)

The local feature size at a point $x \in \mathcal{M}$ is its distance to the medial axis of $\mathcal{M}$.

ϵ-sample

A set of points P on $\mathcal{M}$ such that $\forall x \in \mathcal{M}\ \exists p \in P$ s.t. $||px|| \leq \epsilon \cdot lfs(x)$.

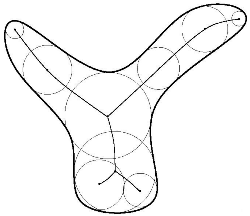

Medial Axis
Figure from [Wolter]

From balls to surfaces [Chazal, Lieutier]

Let P be an ϵ-sample of $\mathcal{M}$, with $\epsilon < 1/160$, and define b_p as the ball centered at $p \in P$ with radius $\alpha_p \cdot lfs(p)$, where $1/20 < \alpha_p < 1/10$. Then, $\mathcal{M}$ is a deformation retraction of $\cup b_p$.

Beyond Homeomorphism: Isotopic Equivalence

 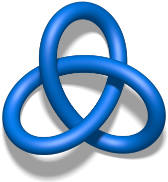

Torus: unknot vs. knot
Figures from [Wikipedia]

Beyond Homeomorphism: Isotopic Equivalence

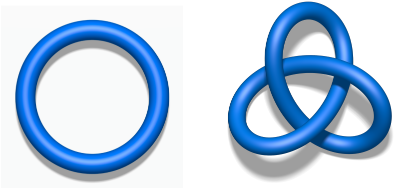

Torus: unknot vs. knot
Figures from [Wikipedia]

A purely topological condition [Chazal, Cohen-Steiner]

Suppose that:

- $\mathcal{M}'$ is homeomorphic to $\mathcal{M}$,
- $\mathcal{M}'$ is included in a topological thickening $\mathbb{M}$ of $\mathcal{M}$,
- $\mathcal{M}'$ separates the sides of $\mathbb{M}$.

Then, $\mathcal{M}'$ is isotopic to $\mathcal{M}$ in $\mathbb{M}$.

VoroCrust - The Abstract Algorithm

- Start with an ϵ-sample $P \subset \mathcal{M}$ with weights ($\delta \geq \epsilon$) defining the associated δ-lfs balls B.

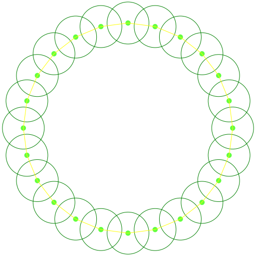

VoroCrust - The Abstract Algorithm

- Start with an ϵ-sample $P \subset \mathcal{M}$ with weights ($\delta \geq \epsilon$) defining the associated δ-lfs balls B.
- Collect the corner points $\mathcal{G}$ of $\cup B$ as a crude set of witnesses of the simplices in $\mathcal{K}$.

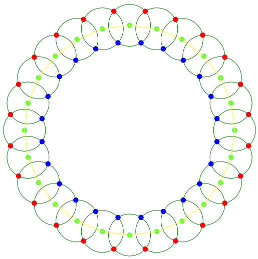

VoroCrust - The Abstract Algorithm

- Start with an ϵ-sample $P \subset \mathcal{M}$ with weights ($\delta \geq \epsilon$) defining the associated δ-lfs balls B.
- Collect the corner points $\mathcal{G}$ of $\cup B$ as a crude set of witnesses of the simplices in $\mathcal{K}$.
- Compute the Voronoi diagram of $\mathcal{G}$, $Vor(\mathcal{G})$.

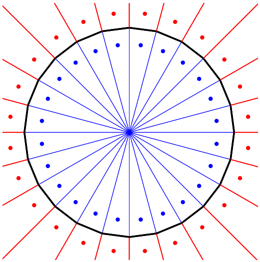

VoroCrust - The Abstract Algorithm

- Start with an ϵ-sample $P \subset \mathcal{M}$ with weights ($\delta \geq \epsilon$) defining the associated δ-lfs balls B.
- Collect the corner points $\mathcal{G}$ of $\cup B$ as a crude set of witnesses of the simplices in $\mathcal{K}$.
- Compute the Voronoi diagram of $\mathcal{G}$, $Vor(\mathcal{G})$.
- Produce the surface approximation as the facets of $Vor(\mathcal{G})$ separating interior/exterior corners; we call this the VoroCrust of $\mathcal{G}$ (VC).

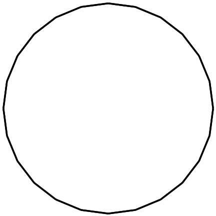

VoroCrust - The Abstract Algorithm

- Start with an ϵ-sample $P \subset \mathcal{M}$ with weights ($\delta \geq \epsilon$) defining the associated δ-lfs balls B.
- Collect the corner points $\mathcal{G}$ of $\cup B$ as a crude set of witnesses of the simplices in $\mathcal{K}$.
- Compute the Voronoi diagram of $\mathcal{G}$, $Vor(\mathcal{G})$.
- Produce the surface approximation as the facets of $Vor(\mathcal{G})$ separating interior/exterior corners; we call this the VoroCrust of $\mathcal{G}$ (VC).
- Include in $\mathcal{G}$ more samples from the volume bounded by $\mathcal{M}$ to further decompose it.

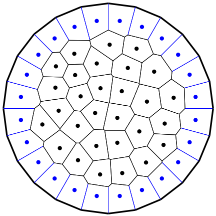

VoroCrust - The Abstract Algorithm

- Start with an ϵ-sample $P \subset \mathcal{M}$ with weights ($\delta \geq \epsilon$) defining the associated δ-lfs balls B.
- Collect the corner points $\mathcal{G}$ of $\cup B$ as a crude set of witnesses of the simplices in $\mathcal{K}$.
- Compute the Voronoi diagram of $\mathcal{G}$, $Vor(\mathcal{G})$.
- Produce the surface approximation as the facets of $Vor(\mathcal{G})$ separating interior/exterior corners; we call this the VoroCrust of $\mathcal{G}$ (VC).
- Include in $\mathcal{G}$ more samples from the volume bounded by $\mathcal{M}$ to further decompose it.

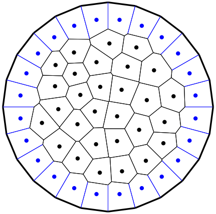

Sandwich theorem

$$VC \subseteq \mathcal{S} \subseteq \cup B.$$

VoroCrust - Ball Intersections

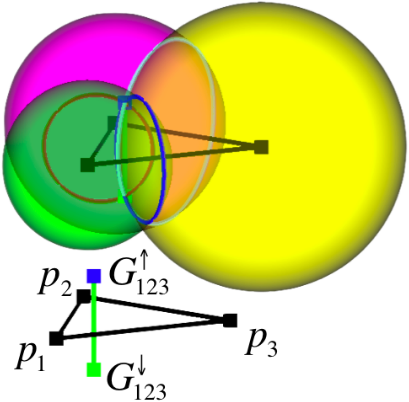

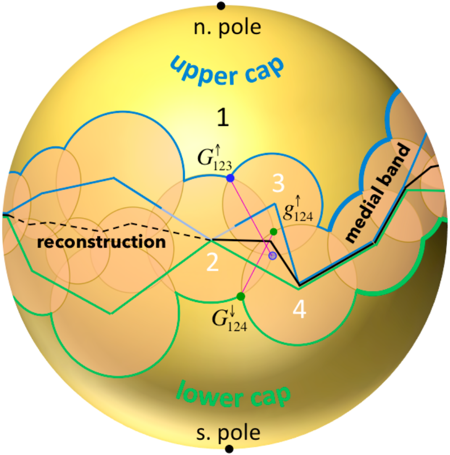

VoroCrust - Sampling Conditions for Disk Caps

Disk Caps

Each sample ball contributes exactly two caps, i.e., topological-disks, to the boundary of the union.

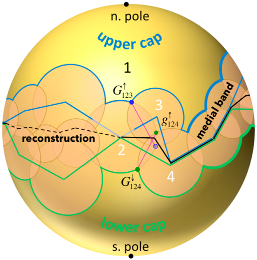

VoroCrust - Sampling Conditions for Disk Caps

Disk Caps

Each sample ball contributes exactly two caps, i.e., topological-disks, to the boundary of the union.

Sampling Conditions

For constants $\epsilon \leq \delta$, we require an ϵ-sampling P, with associated balls of radii $r_i = \delta \cdot lfs(p_i)$ satisfying the following sparsity condition:

$$lfs(q) \geq lfs(p) \implies \|p - q\| \geq \epsilon \cdot lfs(p).$$

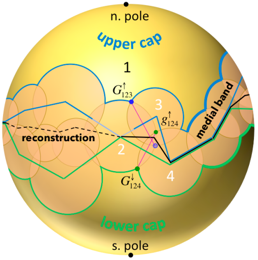

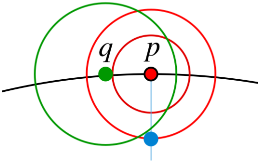

VoroCrust - Sampling Conditions for Disk Caps

Disk Caps

Each sample ball contributes exactly two caps, i.e., topological-disks, to the boundary of the union.

Sampling Conditions

For constants $\epsilon \leq \delta$, we require an ϵ-sampling P, with associated balls of radii $r_i = \delta \cdot lfs(p_i)$ satisfying the following sparsity condition:

$$lfs(q) \geq lfs(p) \implies \|p - q\| \geq \epsilon \cdot lfs(p).$$

Lemma

Taking $\epsilon = 1/160$ and $\delta = 1/20$, we get disk caps.

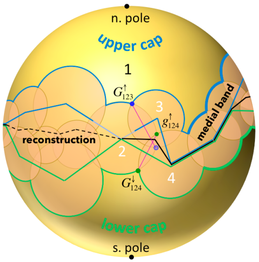

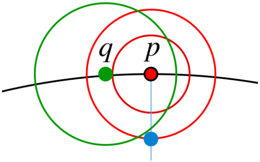

VoroCrust - Sample Results

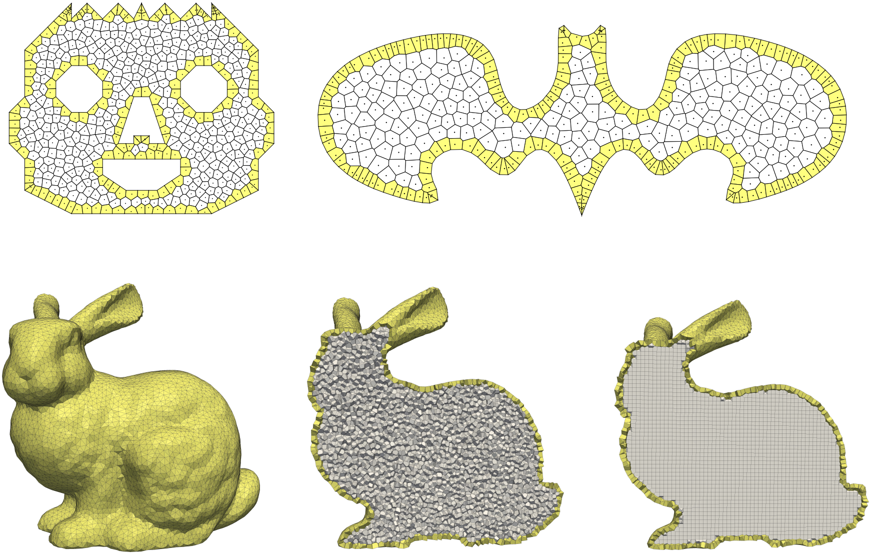

Announcements

- The VoroCrust software package is scheduled for release soon.
  - Successful implementation of more ideas than what this talk covers, e.g., sharp features, medial axis approximation, sizing estimation.
- Mohamed S. Ebeida (msebeid@sandia.gov) is the VoroCrust point-of-contact at Sandia National Labs (SNL).